A&A 404, 495–504 (2003)
DOI: 10.1051/0004-6361:20030479

Astronomy & Astrophysics

CI and CO in the nearby spiral galaxies IC 342 and Maffei 2

F. P. Israel[1] and F. Baas[1,2,⋆]

[1] Sterrewacht Leiden, PO Box 9513, 2300 RA Leiden, The Netherlands
[2] Joint Astronomy Centre, 660 N. A'ohoku Pl., Hilo, Hawaii, 96720, USA

Received 19 February 2003 / Accepted 27 March 2003

Abstract. We present $J = 2–1$, $J = 3–2$, $J = 4–3$ ^{12}CO and 492 GHz [CI] maps as well as $J = 2–1$ and $J = 3–2$ ^{13}CO measurements of the central regions in the nearby Sc galaxies IC 342 and Maffei 2. In both galaxies, the distribution of CO and [CI] is strongly concentrated towards the center. These centers harbour modest starbursts. Both galaxies have nearly identical ^{12}CO transitional ratios but the relative intensities of their ^{13}CO and [CI] emission lines differ significantly. The observed sets of line intensities require modelling with a multi-component molecular gas. In both galaxies, a dense component must be present ($n(H_2) \approx 10^4–10^5$ cm^{-3}) with kinetic temperatures $T_{kin} = 10–20$ K (IC 342) or 20–60 K (Maffei 2), as well as a less dense (IC 342: a few hundred cm^{-3} at most; Maffei 2: $\approx 3 \times 10^3$ cm^{-3}) and hotter ($T_{kin} = 100–150$ K) component. In both galaxies, neutral and ionized atomic carbon amounts are between 1.5 and 2.5 times those of CO. In both starburst centers about half to two thirds of the molecular gas mass is associated with the hot PDR phase. The center of IC 342 contains within $R = 0.25$ kpc an (atomic and molecular) gas mass of 1×10^7 $M_\odot$ and a peak face-on gas mass density of about 70 $M_\odot$ pc^{-2}. For Maffei 2 these numbers are less clearly defined, mainly because of uncertainties in its distance and carbon abundance. We find a gass mass $M_{gas} \geq 0.5 \times 10^7$ $M_\odot$, and a peak face-on gas mass density of about 35 $M_\odot$ pc^{-2}.

Key words. galaxies: individual: IC 342; Maffei 2 – galaxies: ISM – radio lines: galaxies – ISM: molecules

1. Introduction

Molecular gas is a major constituent of the interstellar medium in galaxies. Within the inner kiloparsec, many spiral galaxies exhibit a strong concentration of molecular gas towards their nucleus. We have conducted a programme to observe a number of nearby galaxies in various CO transitions and in the 492 GHz $^3P_1–^3P_0$ CI transition in order to determine the physical condition of such central molecular gas concentrations. Results on NGC 253 (Israel et al. 1995), NGC 7331 (Israel & Baas 1999), NGC 6946 and M 83 = NGC 5236 (Israel & Baas 2001) have already been published. In this paper, we present the results for the very nearby galaxies IC 342 and Maffei 2 whose basic properties are summarized in Table 1.

Both are major members of the IC 342/Maffei group, which is located at a distance of about 2 Mpc (Huchtmeier et al. 2000 and references therein). This appears to be the galaxy group closest to the Local Group but it is, unfortunately, located in the sky very close to the Galactic plane. Consequently, its members suffer high foreground extinction rendering several of them, including Maffei 2, all but invisible at optical wavelengths. Mainly for this reason, the distance of Maffei 2 is still quite uncertain. However, it is usually assumed that it exceeds that of IC 342. We have thus assumed a distance of 2.7 Mpc which is in line with the overall cluster value, but 50 per cent greater than the reasonably well established distance to IC 342. Both IC 342 and Maffei 2 have been studied well at longer wavelengths, including those of the CO line. Inasmuch as IC 342 is, together with NGC 253 and M 82, one of the strongest (sub)millimeter line emitters in the sky, it has been observed frequently. In the $J = 1–0$ transition of ^{12}CO, it was one of the first galaxies mapped at $\approx 1'$ resolution (Morris & Lo 1978; Rickard & Palmer 1981; Young & Scoville 1982). More extensive mapping of the ^{12}CO and ^{13}CO isotopes in both the $J = 1–0$ and $J = 2–1$ transitions was presented by Eckart et al. (1990) and Xie et al. (1994). Emission in the $J = 3–2$ transition was detected and mapped by Ho et al. (1987), Steppe et al. (1990) and Irwin & Avery (1992), while the ^{13}CO isotope was detected in this transition by Wall & Jaffe (1990) and Mauersberger et al. (1999). Finally, the $J = 4–3$ and, with a somewhat uncertain calibration, the $J = 6–5$ ^{12}CO transitions were detected by Güsten et al. (1993) and Harris et al. (1991). The ^{12}CO/^{13}CO isotope ratio was determined to be ≥30 by Henkel et al. (1998). High-resolution aperture synthesis maps of IC 342 have been published in $J = 1–0$ ^{12}CO and ^{13}CO by Ishizuki et al. (1990), Turner & Hurt (1992), Wright et al. (1993) and Sakamoto et al. (1999), and in $J = 2–1$ ^{12}CO and ^{13}CO by Turner et al. (1993) and Meier et al. (2000).

Maffei 2 was first detected in ^{12}CO by Rickard et al. (1977) and subsequently mapped at 23″ resolution by Weliachew et al. (1988). Emission in the $J = 2–1$ and $J = 3–2$ transitions was

Send offprint requests to: F. P. Israel,
e-mail: israel@strw.leidenuniv.nl
⋆ Deceased April 4, 2001.

Table 1. Galaxy parameters.

	IC 342	Maffei 2
Type[a]	SABcd	SABbc
Optical Centre:		
RA (B1950)[b]	$03^h41^m58.6^s$	$02^h38^m08.0^s$
Dec (B1950)[b]	$+67°56'26''$	$+59°23'24''$
RA (J2000)	$03^h46^m49.7^s$	$02^h41^m54.6^s$
Dec (J2000)	$+68°05'45''$	$+59°36'11''$
Radio Centre:		
RA (B1950)[c]	$03^h41^m57.3^s$	$02^h38^m08.4^s$
Dec (B1950)[c]	$+67°56'27''$	$+59°23'30''$
$V_{LSR}^{c,d}$	$+35$ km s^{-1}	-31 km s^{-1}
Inclination i^d	25°	67°
Position angle P^d	39°	26°
Distance D^e	1.8 Mpc	2.7 Mpc
Luminosity L_B^f	$2\times10^{10}\ L_{B\odot}$	$1\times10^{10}\ L_{B\odot}$
Scale	115 ″/kpc	77 ″/kpc

Notes to Table 1:
[a] RSA (Sandage & Tammann 1987);
[b] Dressel & Condon (1976);
[c] Hummel & Gräve (1990); Turner & Ho (1994);
[d] Rots (1979); Newton (1980); Hurt et al. (1996);
[e] McCall (1989) for IC 342; for Maffei 2 see text;
[f] Buta & McCall (1999), assuming Galactic foreground for IC 342 $A_B = 3.32$ mag (Madore & Freedman 1992); for Maffei 2 an uncertain foreground $A_B = 8$ mag is assumed.

measured by Wall et al. (1993) and Mauersberger et al. (1999). Maffei 2 was mapped in $J = 1{-}0$ ^{12}CO and ^{13}CO by Ishiguro et al. (1989) and Hurt & Turner (1991), in $J = 2{-}1$ ^{12}CO by Sargent et al. (1985) and in $J = 3{-}2$ ^{12}CO by Hurt et al. (1993).

Although the molecular line emission from Maffei 2 is somewhat weaker than that from IC 342, both are frequently included in the same observing programs. Both have been observed in a great variety of other molecular species: CS (Mauersberger & Henkel 1989; Mauersberger et al. 1989; Sage et al. 1990; Paglione et al. 1995), HCN and HCO^+ (Nguyen-Q-Rieu et al. 1992; Downes et al. 1992; Jackson et al. 1995; Paglione et al. 1997), $H^{13}CO^+$ and N_2H^+ (Mauersberger & Henkel 1991); HNC (Hüttemeister et al. 1995), CN and HC_3N (Henkel et al. 1988), HNCO (Nguyen-Q-Rieu et al. 1991), OCS (Mauersberger et al. 1995) as well as H_2CO and CH_3OH (Hüttemeister et al. 1997). In particular the discovery of strong NH_3 emission, first from IC 342 (Ho et al. 1990 and references therein), then from Maffei 2 (Henkel et al. 2000; Takano et al. 2000) showed that a significant fraction of the molecular gas in the centers of these galaxies is both dense and hot.

2. Observations

All observations described in this paper were carried out with the 15 m James Clerk Maxwell Telescope (JCMT) on Mauna Kea (Hawaii)[1]. Details are given in Table 2. Up to 1993, we used a 2048 channel AOS backend covering a band of 500 MHz (650 km s^{-1} at 230 GHz). After that year, the DAS digital autocorrelator system was used in bands of 500 and 750 MHz. Integration times given in Table 2 are typical values used in mapping; central positions were usually observed more than once and thus generally have significantly longer integration times. Values listed are on+off. When sufficient free baseline was available, we subtracted second or third order baselines from the profiles. In all other cases, linear baseline corrections were applied. All spectra were scaled to a main-beam brightness temperature, $T_{mb} = T_A^*/\eta_{mb}$; relevant values for η_{mb} are given in Table 2. Spectra of the central positions in both galaxies are shown in Fig. 1 and summarized in Table 3. In Table 2, we have also listed the parameters describing the various maps obtained. All maps are close to fully sampled. In all maps, the mapping grid was rotated by the angle given in Table 2 so that the Y axis coincided with the galaxy major axis. The velocity-integrated maps shown in Figs. 2 and 3 have been rotated back, so that north is (again) at top and the coordinates are right ascension and declination. For IC 342, the map grid origin in the $J = 2{-}1$ and $J = 3{-}2$ CO maps is within a few arcseconds from the optical centre listed in Table 1, whereas the $J = 4{-}3$ and [CI] maps find their origin close to the radio centre; the two sets of maps are thus offset from one another by $\Delta\alpha$, $\Delta\delta = +9''$, $-3''$. For Maffei 2, the grid origin is again close to the optical centre; the radio centre occurs in the maps nominally at $\Delta\alpha$, $\Delta\delta = -0.8''$, $+6''$.

3. Results

3.1. CO distribution

In both galaxies, molecular gas as traced by CO is strongly concentrated towards the center. The central molecular source is contained with $R < 250$ pc in the case of IC 342, and $R < 200 \times D/2.7$ pc in the case of Maffei 2, where D is the true distance of Maffei 2 in Mpc.

CO line aperture synthesis maps of IC 342 show, at resolutions of $2''{-}4''$, considerable structure only hinted at in our maps (Fig. 2). Clearly, the central CO concentration is not toroidal in shape. Rather, the maps published by Sakamoto et al. (1999) and Meier et al. (2000) show individual CO peaks (cloud complexes) distributed along a perspectively foreshortened double spiral – although the foreshortening seems more than expected for an inclination of only 25°. The molecular gas enhancement of spiral arms ends at about $R = 250$ pc from the nucleus. The nucleus itself is located at a minimum in the CO distribution. Emission from the high-density tracer HCN offers a very similar appearance (Downes et al. 1992). Our $J = 2{-}1$ ^{12}CO map shows an elongated source, in which a smoothed version of the high-resolution map by Meier et al. (2000) is easily recognized. Emission in all our CO maps, as well as the [CI] map peaks at the position coinciding with cloud complex B in the designation by Downes et al. (1992). This peak becomes more pronounced with increasing J level, and in [CI]. This is partly the consequence of increasing angular resolution,

[1] The James Clerk Maxwell Telescope is operated on a joint basis between the United Kingdom Particle Physics and Astrophysics Council (PPARC), the Netherlands Organisation for Scientific Research (NWO) and the National Research Council of Canada (NRC).

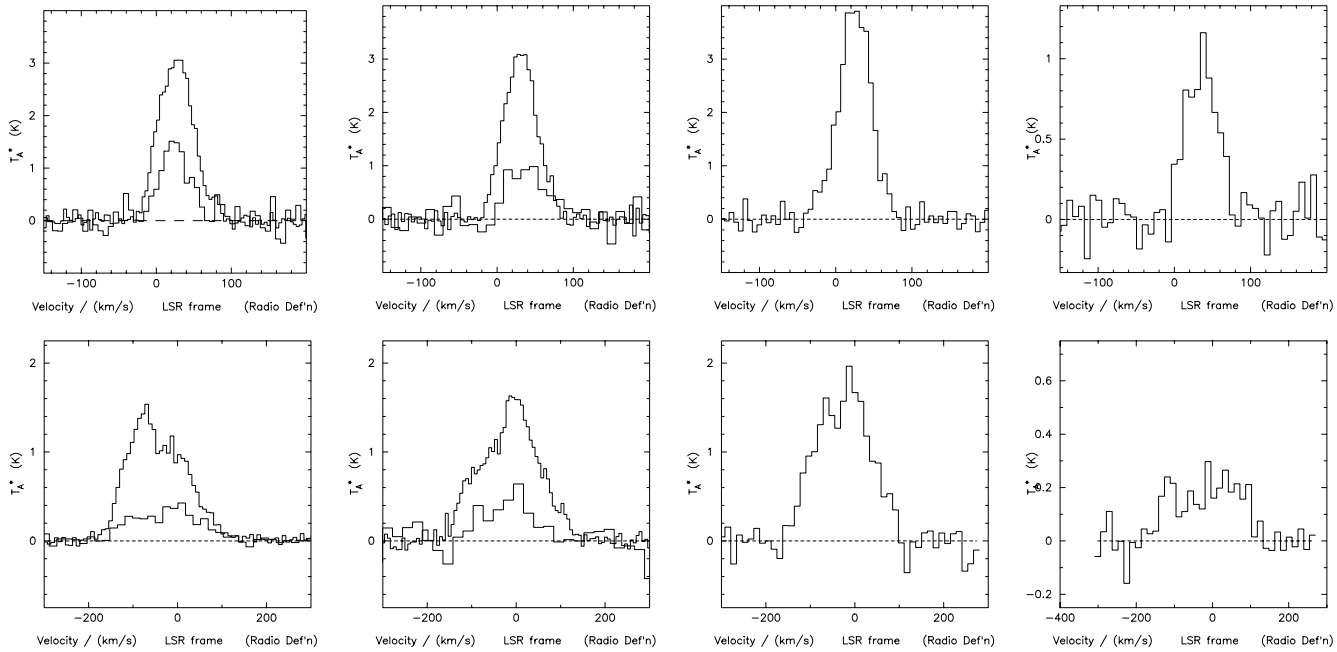

Fig. 1. Full resolution emission-line spectra observed towards the centers of IC 342 and Maffei 2. Top row: IC 342; bottom row: Maffei 2. Columns from left to right: $J = 2{-}1$ CO, $J = 3{-}2$ CO, $J = 4{-}3$ CO, [CI]. Vertical scale is actually in $T_{\rm mb}$. Whenever available, ^{13}CO profiles are shown as the lower of the two profiles in the appropriate ^{12}CO box. Their brightness temperatures have been multiplied by three, so that they are depicted on the same temperature scale as [CI] in the right hand boxes.

Table 2. Observations Log.

Transition	Object	Date	Freq	$T_{\rm sys}$	Beam Size	$\eta_{\rm mb}$	t(int)	Map Parameters			
								Points	Size	Spacing	PA
		(MM/YY)	(GHz)	(K)	(″)		(s)		(″)	(″)	(°)
^{12}CO $J = 2{-}1$	IC 342	02/89	230	1290	21	0.63	600	16	40×80	8	70
		01/96		640		0.69	60	52			
	Maffei 2	01/96		490		0.69	240	25	48×60	12	25
^{12}CO $J = 3{-}2$	IC 342	04/94	345	735	14	0.58	180	39	32×72	8	70
	Maffei 2	12/93		1854		0.53	400	10	36×48	6	27
		11/94		1465		0.58	240	33			
		12/00		565		0.63	120	77	60×80	8	27
^{12}CO $J = 4{-}3$	IC 342	12/93	461	8000	11	0.53	600	8	24×40	8	70
		04/94		2170		0.53	400	14			
	Maffei 2	04/94		3200		0.53	480	7	30×36	6	25
		07/96		3700		0.53	360	26			
^{13}CO $J = 2{-}1$	IC 342	02-89	220	1440	21	0.63	900	5	30×30	15	0
	Maffei 2	01-96		550		0.69	2400	1			
^{13}CO $J = 3{-}2$	IC 342	04-94	330	2170	14	0.58	6000	1			
		01-96		1660		0.58	1560	5	16×16	8	0
	Maffei 2	01-96		2800		0.58	2400	1			
CI $^3P_1{-}^3P_0$	IC 342	11-94	492	5250	10	0.53	800	27	24×48	8	70
	Maffei 2	12-93		4885		0.53	3200	1			

but we also note that the peak coincides with the strongest concentration of thermal radio continuum emission (Turner & Ho 1983), thus with the region containing the highest spatial density of early type stars. The peak line intensities in Table 3 and the line ratios in Table 4 refer to this maximum. We thus expect them to exhibit properties commensurate with a starburst environment, i.e. those of a photon-dominated region (PDR).

The region corresponding to complexes C and D (Downes et al. 1992), referred to as "Eastern Ridge" by Eckart et al. (1990), behaves differently. It is almost as pronounced as region B in the $J = 2{-}1$ transition, but fades rapidly at higher J levels. Its molecular gas must thus be cooler on the whole than that of region B. This is, in any case, consistent with the much less impressive appearance of this region in the radio

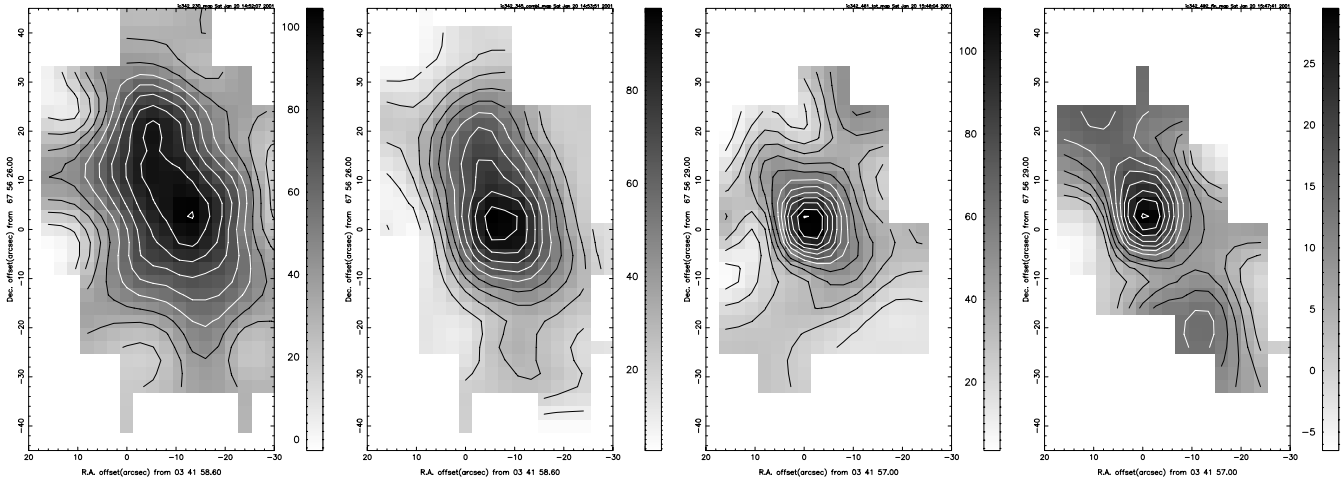

Fig. 2. Contour maps of emission from IC 342 integrated over the velocity range $V_{\rm LSR} = -100$ to 200 km s^{-1}. North is at top. Offsets are marked in arcminutes with respect to J2000 coordinates $\alpha_\circ = 03^{\rm h}46^{\rm m}49.^{\rm s}7, \delta_\circ = +68°05'45''$. Left to right: CO $J = 2$–1, CO $J = 3$–2, CO $J = 4$–3 and [CI]. Contour values are linear in $\int T_{\rm mb}{\rm d}V$. Contour steps are 16 K kms^{-1} (2–1, 3–2, 4–3) and 5 K kms^{-1} (CI) and start at step 1.

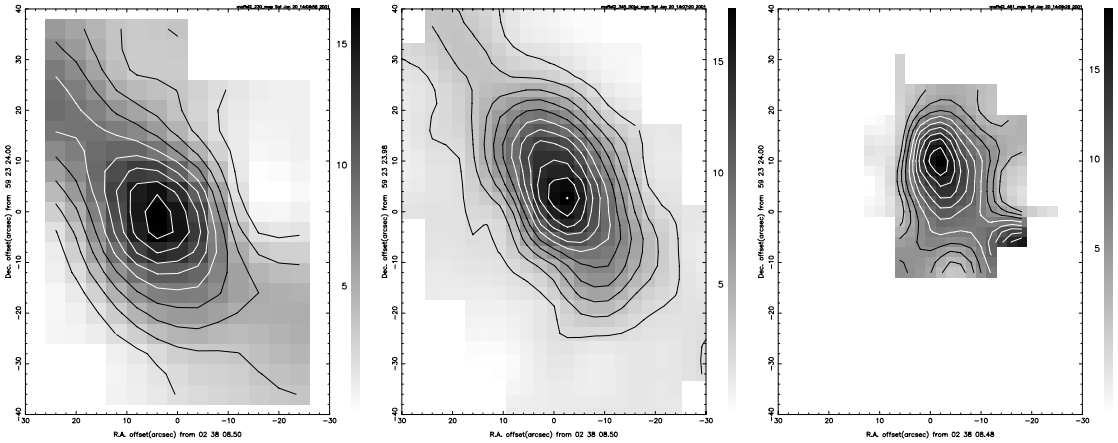

Fig. 3. Contour maps of emission from Maffei 2 integrated over the velocity range $V_{\rm LSR} = -200$ to +150 km s^{-1}. North is at top. Offsets are marked in arcminutes with respect to J2000 coordinates $\alpha_\circ = 02^{\rm h}41^{\rm m}54.^{\rm s}6, \delta_\circ = +59°36'11''$. Left to right: CO $J = 2$–1, CO $J = 3$–2, CO $J = 4$–3. Contour values are linear in $\int T_{\rm mb}{\rm d}V$. Contour steps are 25 K kms^{-1} (2–1 and 3–2) and 35 K kms^{-1} (4–3) and start at step 1.

Table 3. Central CO and CI line intensities in IC 342 and Maffei 2.

Transition			IC 342			Maffei 2		
		Resolution	$T_{\rm mb}{}^a$	$\int T_{\rm mb}{\rm d}V^a$	$L_{\rm tot}{}^b$	$T_{\rm mb}{}^a$	$\int T_{\rm mb}{\rm d}V^a$	$L_{\rm tot}{}^b$
		($''$)	(mK)	(K kms^{-1})	K kms^{-1} kpc^2	(mK)	(K kms^{-1})	K kms^{-1} kpc^2
^{12}CO	$J = 2$–1	21	3090	172 ± 19	15.4	1500	245 ± 35	11.6
		43		98 ± 14			106 ± 15	
	$J = 3$–2	14	3140	186 ± 23	10.4	1650	295 ± 35	7.6
		21		126 ± 13			165 ± 15	
	$J = 4$–3	11	4020	209 ± 21	4.6	1950	405 ± 50	5.7
		14		176 ± 19			280 ± 35	
		21		115 ± 14			160 ± 25	
^{13}CO	$J = 2$–1	21	476	24.0 ± 3	—	150	22 ± 4	—
		43		12.0 ± 2			—	
	$J = 3$–2	14	311	17.1 ± 2	—	200	20 ± 4	—
		21		14.4 ± 2			—	
[CI]	$^3P_1$–$^3P_0$	10	1030	54 ± 6	1.0	190	37 ± 7	—
		14		42 ± 8			—	
		21		27 ± 7			—	

[a] Beam centered on nucleus.

[b] Total central concentration.

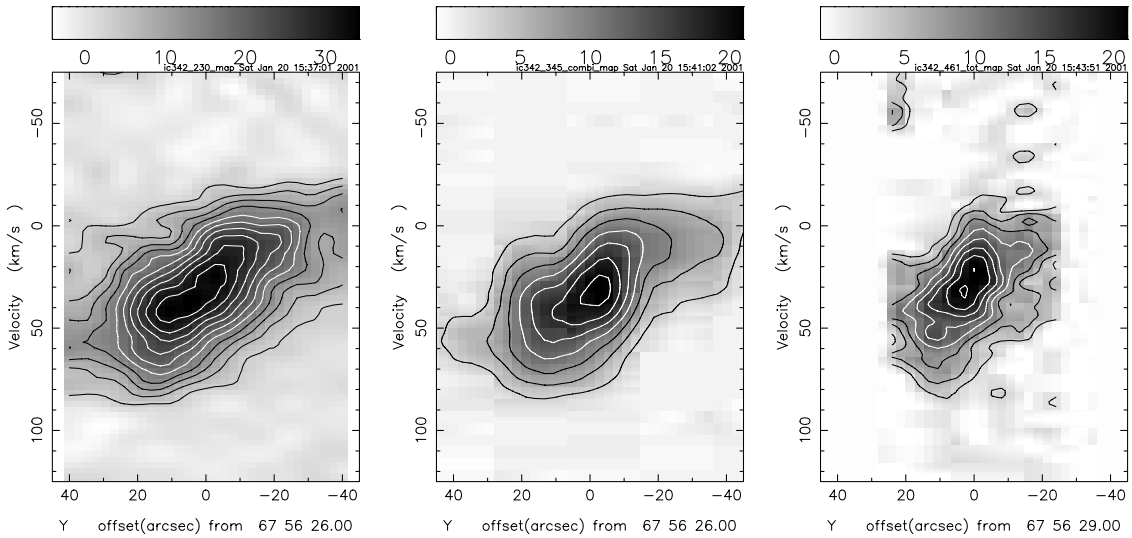

Fig. 4. Position-velocity maps of CO emission from IC 342 in position angle 20°. Left to right: CO $J = 2–1$, CO $J = 3–2$ and CO $J = 4–3$. Contour values are linear in $T_{\rm mb}$. All maps are one beamwidth wide, have a velocity resolution of 7.5 km s^{-1} and have contour steps of 5 K, starting at step 1. Vertical scale is $V_{\rm LSR}$.

Table 4. Integrated line ratios in the centres of IC 342 and Maffei 2.

Transitions	IC 342		Maffei 2	
	Nucleus	Total Center	Nucleus	Total Center
^{12}CO (1–0)/(2–1)[a]	0.95 ± 0.1	0.9	0.9 ± 0.2	0.8:
^{12}CO (3–2)/(2–1)[b]	0.73 ± 0.10	0.7	0.75 ± 0.13	0.7
^{12}CO (4–3)/(2–1)[b]	0.67 ± 0.10	0.3	0.65 ± 0.10	0.5
^{12}CO/^{13}CO (1–0)[c]	10.7 ± 1.3	—	8.6 ± 1.1	—
^{12}CO/^{13}CO (2–1)[b]	7.2 ± 1.5	—	10.0 ± 1.4	—
^{12}CO/^{13}CO (3–2)[d]	10.2 ± 1.4	—	12.4 ± 1.7	—
CI/CO(2–1)[b]	0.16 ± 0.03	0.06	0.10 ± 0.05	—
CII/CO(2–1)[e]	0.54		0.31	

[a] IC 342 ratio from Eckart et al. (1990), Xie et al. (1994) and Meier et al. (2000); Maffei 2 ratio from $J = 1–0$ data by Weliachew et al. (1988); both ratios at 21″ resolution; [b] This Paper, JCMT at 21″ resolution; [c] Weighted mean based on ratios presented by Rickard & Blitz (1985); NRAO at 65″ resolution; Young & Sanders (1986); FCRAO at 45″ resolution; Weliachew et al. (1988); IRAM 30 m at 24″ resolution; Sage & Isbell (1991); NRAO 12m at 57″ resolution; Xie et al. (1994) FCRAO at 45″ resolution; Meier et al. (2000) OVRO at 4.″5 resolution; [d] This Paper; JCMT at 14″ resolution; [e] From Crawford et al. (1985) and Stacey et al. (1991), KAO at 55″ resolution; JCMT convolved to 55″ resolution.

continuum maps by Turner & Ho (1983). There appear to be relatively weak, secondary maxima in the neutral carbon emission at the northern and southern edges of the main CO distribution, in addition to the primary [CI] maximum at cloud B.

The major-axis position-velocity map of IC 342 covers a relatively small velocity range, in accordance with the mostly face-on orientation of the galaxy. With increasing J level, hence increasing resolution and decreasing beamsmearing, the rotation steepens. In the $J = 4–3$ CO p-V map the central material covers a range of about 80 km s^{-1} over about 20″. The rotation in this region is characterized by a velocity gradient (cf. $J = 4–3$ CO in Fig. 4 and $J = 1–0$ CO in Fig. 4 of Sakamoto et al. 1999) $\mathrm{d}V/\mathrm{d}\theta = 7.8$ km s^{-1}/″, corresponding to $\mathrm{d}V/\mathrm{d}R \approx 2.1$ km s^{-1}/pc in the plane of the galaxy.

The structure of the central CO source in Maffei 2 is more complex than Fig. 3 suggests. The galaxy is much more tilted than IC 342, and the integrated velocity images, showing only a resolved but featureless central source, are misleading. Maps of peak temperature $T_{\rm mb}$ rather than integrated-velocity temperature maps show a distinct double-peaked source (see also Hurt et al. 1993). This is in sharp contrast to IC 342, where peak-temperature and integrated-temperature maps show only marginally different morphologies. The deceptively simple appearance of Maffei 2 in Fig. 3 is easily explained by a glance at the major axis position-velocity maps in Fig. 5. The single peak in the integrated map results from the line-of-sight superposition of two distinct velocity components. This is, in fact, the same situation that we found to apply to NGC 253 (Israel et al. 1995), and it is one to watch out for in all high-inclination galaxies. The CO source in Fig. 3 becomes more compact with increasing J level, i.e. increasing frequency. As can be seen in Fig. 5, this is mostly the consequence of increasing resolution and decreasing beamsmearing. In the peak-temperature maps (not shown) the separation of the two peaks is only 13″ (corresponding to 170 pc). The CO distribution shown in Figs. 3 and 5 is characteristic for a toroidal distribution of molecular

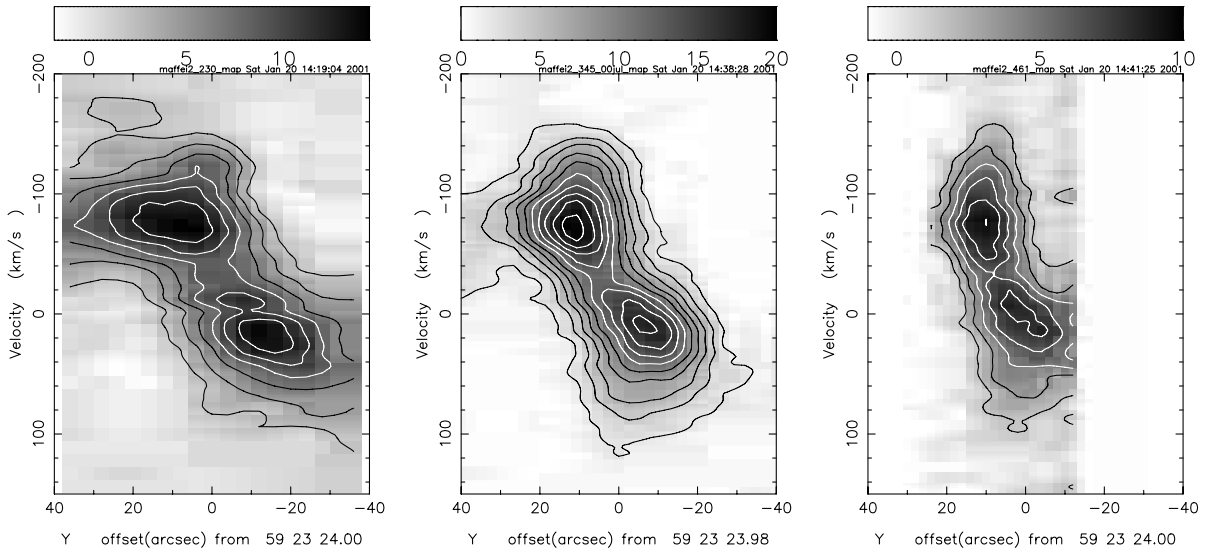

Fig. 5. Position-velocity maps of CO emission from Maffei 2 in position angle 25°. Left to right: CO $J = 2{-}1$, CO $J = 3{-}2$ and CO $J = 4{-}3$. Contour values are linear in $T_{\rm mb}$. All maps are one beamwidth wide, have a velocity resolution of 10 km s^{-1} and have contour steps of 3 K, starting at step 1. Vertical scale is $V_{\rm LSR}$.

gas, with a 45–60 pc wide gap in the center. However, the "S"-shaped morphology of CO in high-resolution (6″) aperture synthesis maps by Ishiguro et al. (1989) and Hurt & Turner (1991) strongly suggests greatly enhanced emission from molecular gas in inner spiral arms instead.

The effects of beamsmearing are quite noticeable in the p-V maps in Fig. 5. The average velocity gradient increases from 4.5 km s^{-1}/″ in the $J = 2{-}1$ CO map to about 18 km s^{-1}/″ in the $J = 4{-}3$ CO map. The latter value corresponds to dV/dR = 1.4 km s^{-1}/pc, i.e. not much different from the gradient in IC 342 (or NGC 6946 and M 83 for that matter – see Israel & Baas 2001). We note that the CO distribution in Fig. 5 just fills the steep leading edge of the major axis HI distribution in Maffei 2 (Fig. 9 in Hurt et al. 1996).

3.2. Line ratios

We have determined the intensity ratio of the observed transitions at the centers of both galaxies; all intensities are normalized to those of the $J = 2{-}1$ ^{12}CO line. The columns in Table 4 marked "Nucleus" refer to ratios in a 21″ beam centered on the nucleus, with the exception of the [CII]/CO(2–1) ratio which was determined after convolution of the $J = 2{-}1$ ^{12}CO measurements to the 55″ beam of the [CII] observations, and the $J = 1 - 0$ ^{12}CO/^{13}CO isotopic ratio which represents a weighted mean from a number of determinations at various resolutions. The [CII] intensities (Crawford et al. 1985; Stacey et al. 1991), were converted to velocity-integrated temperatures to obtain the line ratios in Table 4. The columns marked "Total Center" refer to the intensities of the central concentration integrated over the source extent in the maps. The apparent decrease in source extent going from the lower J levels (lower frequencies) to the higher frequencies is mostly an artifact of limited resolution. When corrected for finite beamwidth, source dimensions at e.g. the $J = 2{-}1$ and $J = 4{-}3$ transitions are in fact very similar. Nevertheless, the smaller area coverage in the [CI] and $J = 4{-}3$ CO maps may ahve led to an underestimate of the total intensity. The entries in Table 4 suggest that this may indeed be the case. The $J = 1{-}0/J = 2{-}1$ ratios have relatively large uncertainties, because we could not use observations of our own, but instead have used estimated $J = 1{-}0$ intensities reduced to a 21″ beam from the references given in the table. These ratios are, in any case, close to unity.

The ^{12}CO ratios are quite similar for both galaxies, but the intensity of the [CI] and [CII] lines relative to CO is significantly lower in Maffei 2 than in IC 342, suggesting stronger PDR effects in the latter. The intensity of the [CII] line indicates the presence of both high temperatures and high gas densities in the medium as the critical values for this transition are $T_{\rm kin} \geq 91$ K and $n \geq 3500$ cm^{-3}. At the same time, such values must be reconciled with the much lower temperatures and (column) densities implied by the more modest isotopic ratios in the lower CO transitions. These isotopic ratios differ for the two galaxies. For each individual transition the isotopic ratios just agree within the errors, but the overall patterns are clearly different. For Maffei 2, the isotopic ratio increases with increasing J level, but for IC 342 the isotopic ratio is minimal in the $J = 2{-}1$ transition. These differences suggest significant differences in the molecular gas properties at the positions sampled in both galaxies

4. Analysis

4.1. Modelling of CO

The observed ^{12}CO and ^{13}CO line intensities and ratios have been modelled with the large-velocity gradient (LVG) radiative transfer models described by Jansen (1995) and Jansen et al. (1994). These provide model line intensities as a function of three input parameters: gas kinetic temperature $T_{\rm k}$, molecular hydrogen density $n(H_2)$ and CO column density per unit velocity (N(CO)/dV). By comparing model line *ratios* to the

Table 5. Model parameters.

Model	Component 1			Component 2			Relative
	Kinetic temperature T_k (K)	Gas density $n(H_2)$ (cm^{-3})	CO column density $N(CO)/dV$ (cm^{-2} $(km\,s^{-1})^{-1}$)	Kinetic temperature T_k (K)	Gas density $n(H_2)$ (cm^{-3})	CO column density $N(CO)/dV$ (cm^{-2} $(km\,s^{-1})^{-1}$)	$J = 2-1$ ^{12}CO emission component 1:2
			IC 342				
1	150	1000	3×10^{17}	150	3000	0.6×10^{17}	0.65 : 0.35
2	100	1000	3×10^{17}	100	3000	1×10^{17}	0.35 : 0.65
3	10	10 000	3×10^{17}	100	3000	1×10^{17}	0.25 : 0.75
			Maffei 2				
4	150	500	10×10^{17}	150	3000	0.3×10^{17}	0.25 : 0.75
5	150	100	10×10^{17}	60	10 000	0.6×10^{17}	0.50 : 0.50
6	100	100	10×10^{17}	20	100 000	0.3×10^{17}	0.30 : 0.70
7	10	3000	6×10^{17}	150	3000	0.6×10^{17}	0.35 : 0.65

observed ratios we have identified the physical parameters best describing the actual conditions in the observed source. Beam-averaged properties are determined by comparing observed and model intensities. In principle, with seven measured line intensities, properties of a single gas component are overdetermined as only five independent observables are required. We found that no single-component fit could be made to the data of either IC 342 or Maffei 2.

However, good fits based on two gas components can be obtained. In order to reduce the number of free parameters, we assume identical CO isotopical abundances for both gas components and assign the specific value $[^{12}CO]/[^{13}CO] = 40$ (Mauersberger & Henkel 1993; Henkel et al. 1998). We identified acceptable fits by searching a grid of model parameter combinations ($10\ K \le T_k \le 250\ K$, $10^2\ cm^{-3} \le n(H_2) \le 10^5\ cm^{-3}$, $6 \times 10^{15}\ cm^{-2} \le N(CO)/dV \le 3 \times 10^{18}\ cm^{-2}$) for model line ratios matching the observed set, with the relative contribution of the two components as the single free parameter. Largely as a consequence of the non-negligible finite errors in the line ratios, solutions are not unique, but rather delineate a range of values in a particular region of parameter space. To a certain extent, variations in input parameters may compensate for one another, leading to identical line ratios for somewhat different combinations of input parameters. We have rejected all solutions in which the denser gas component is also hotter than the more tenuous component, as we consider this physically unlikely on the linear scales observed. From the remainder of solutions, we have selected characteristic examples and listed these in Table 5.

The line ratios observed for IC 342 allow only a rather limited range of gas parameters. One of the two components has well-determined parameters: a column density $N(CO)/dV = 6-10 \times 10^{16}\ cm^{-2}$, an H_2 density of 3000 cm^{-3}) and a kinetic temperature of 100−150 K. The other gas component either is less dense and equally hot, or denser and much cooler with a temperature of the order of 10−20 K. For Maffei 2, the choice of models is less restricted. Possible solutions pair a low-density, hot component and rather large column densities with a much denser, low-column density component of uncertain temperature. Alternatively, both components have a reasonably high density of 3000 cm^{-3}, but represent either a low temperature/high column-density or a high temperature/low column-density gas.

A further check on the validity of the model results is provided by the $C^{18}O$ measurements obtained by Eckart et al. (1990). This isotope was not included in our modelling requirements. For isotopic ratios between $^{12}CO/C^{18}O = 250$ (model 1) and $^{12}CO/C^{18}O = 225$ (model 3), the parameters of our solutions reproduce the observed intensity ratios in the $J = 1-0$ and $J = 2-1$ transitions within 10%.

4.2. Beam-averaged molecular gas properties

The relation between carbon monoxide, neutral and ionized carbon combines the observed C and C^+ intensities with the chemical models by Van Dishoeck & Black (1988) which show a strong dependence of the $N(C)/N(CO)$ column density ratio on total carbon and molecular hydrogen column densities. In the analysis of [CI], we took the kinetic temperatures, H_2 densities and filling factors resulting from the CO analysis, and then solved for column density $N(CI)$. In practice, the column density of one component is frequently well-determined, whereas that of the other is more or less degenerate. For this reason, we solved for identical velocity dispersions in the two gas components. This procedure we also followed for [CII]; in those cases where both model kinetic temperature and gas density are very different for the two components, we have modelled a *single* [CII] component with the higher kinetic temperature and the higher gas density of the two components. This applies specifically to models 5 and 6 (see below). Finally, we have related total carbon (i.e. C + CO) column densities to molecular hydrogen column densities by using an estimated [C]/[H] gas-phase abundance ratio.

IC 342 has a measured central abundance $[O]/[H] = 2.0 \times 10^{-3}$ (Vila-Costas & Edmunds 1992; Garnett et al. 1997). We are unaware of any abundance determination for Maffei 2,

and therefore use the mean value for the spiral galaxies listed by Zaritzky et al. (1994), [O]/[H] = 1.7×10^{-3}. Then, using the results obtained by Garnett et al. (1999), notably their Figs. 4 and 6, we have estimated carbon abundances [C]/[H] = $1.7 \pm 0.5 \times 10^{-3}$ and $1.45 \pm 0.5 \times 10^{-3}$ for IC 342 and Maffei 2 respectively. As a significant fraction of carbon is tied up in dust particles and thus unavailable in the gas-phase, we have adopted a fractional correction factor $\delta_c = 0.27$ (see for instance van Dishoeck & Black 1988), so that $N_H = [2N(H_2) + N(HI)] = A\,[N(CO) + N(C)]$, where $A = 2200$ and 2500 for IC 342 and Maffei 2 respectively. The numerical parameter A is uncertain by about a factor of two.

In Table 6, we present beam-averaged column densities for both CO and C (C^o and C^+), and H_2 column densities derived under the assumptions just discussed. We also present the total masses estimated to be present in the central molecular concentration calculated from L_{tot} listed in Table 3, and the face-on mass densities implied by hydrogen column density and the galaxy inclination. Notwithstanding the differences between the model cloud parameters, the beam-averaged results in Table 6 are rather similar: hydrogen column densities, masses and mass-densities are well within a factor of two from one another. Beam-averaged *neutral* carbon to carbon monoxide column density ratios range from $N(C^o)/N(CO) = 0.5$–0.6 for IC 342 to $N(C^o)/N(CO) = 0.15$–0.3 for Maffei 2. These values are well within the range found for other late-type galaxies such ad M 82, NGC 253, M 83, and NGC 6946 (White et al. 1994; Israel et al. 1995; Stutzki et al. 1997; Petitpas & Wilson 1998; Israel & Baas 2001).

4.3. The center of IC 342

Even before the model fitting described in the previous section, the center of IC 342 was identified as the abode of hot and dense molecular gas, first by Martin et al. (1982) and Martin & Ho (1985) who found the presence of gas with kinetic temperatures estimated to be 70 K or higher. Somewhat later, measurements of the high-density tracer HCN led Downes et al. (1992) to suspect the presence of molecular gas at various densities in the range $n(H_2) = 150$–3×10^4 cm^{-3} and kinetic temperatures in the range $T_{kin} = 50$–70 K. This gas consisted of a few dense cloud complexes and much less dense gas inbetween. Multitransition HCN measurements (Jackson et al. 1995; Paglione et al. 1997) and other molecules (Paglione et al. 1995; Mauersberger et al. 1995; Hüttemeister et al. 1997; Henkel et al. 2000) suggest kinetic temperatures in the range of 50–200 K, densities of about 10^4 cm^{-3} as well as the presence of additional gas components at lower densities. Such temperatures and densities are not unexpected for the site of a significant burst of star formation (cf. Turner & Ho 1983, 1994). The PDR model calculations by Kaufman et al. (1999), applied to the relative intensities of CO, [CI], [CII] and the far-infrared continuum of the center of IC 342 likewise suggest a temperature $T_{kin} \approx 150$ K, a density around 10^4 cm^{-3} and an ambient radiation field strength $\log G_o = 2.5$ (G_o expressed in units of the Habing Field, i.e. 1.6×10^{-3} erg s^{-1} cm^{-2}. All three model solutions in Table 5 are consistent with these values, although the higher densities suggested by the other molecular line observations are only provided by model 3. More support for model 3 follows from the $C^{18}O$ aperture synthesis observations carried out by Meier & Turner (2001) who find that the molecular cloud complexes have densities of the order of 1000–3000 cm^{-3} and, more importantly, kinetic temperatures of 10–40 K (see also Meier et al. 2000). We thus accept model 3 as the most probable approximation of the physical conditions in the central molecular gas of IC 342. About a third of the total molecular mass resides in a dense, fairly cold component with an excitation temperature close to the kinetic temperature, and very high optical depths in all observed CO transitions; even the ^{13}CO transitions are marginally optically thick with $\tau = 1$–2. Most of the remaining mass is hot, with $T_{ex} = 50$ K. The $J = 1$–0 ^{12}CO transition is optically thin, but the higher transitions are optically thick although optical depths are not extremely high.

Obviously, actual conditions will be more varied and complex, but even then we expect the beam-averaged results to be not very different from the ones obtained here. We find a total central gas mass of about 10^7 $M_\odot$ which agrees well with estimates derived from e.g. HCN observations, but is much lower than the mass values quoted in previous CO studies. However, these were all based on *assumed* CO to H_2 ratios, notably the H_2 column density to CO intensity ratio X. The H_2 column densities and masses presented in this paper are, in contrast, based on total gas-phase carbon amounts and the actual carbon abundance. The uncertainty in these results is essentially determined by the error in the product $\delta_C \times$ [C]/[H], which is hard to quantify, but which we estimate to be about a factor of two. A mass of 10^7 $M_\odot$ is not very high, yet it is about 10% of the dynamical mass with $R = 130$ pc; this renders any value much higher rather unlikely. Model 3 implies for IC 342 a value $X = 3{\times}10^{19}$ H_2 mol cm^{-2}/K kms^{-1}, i.e. almost an order of magnitude lower than commonly used X values for the Galactic Solar Neighbourhood. However, such a low value is not uncommon for a galactic center. We have found similar values for NGC 6946 and M 83 (Israel & Baas 2001), and such values are by now solidly established for the center of our own Milky Way (Sodroski et al. 1995; Oka et al. 1998; Dahmen et al. 1998). As an important consequence of these low values for X and beam-averaged $N(H_2)$, the *abundances of all molecular species* that were derived using erroneously estimated much higher H_2 column densities *must be revised upwards* by almost an order of magnitude. This is particularly important in the case of IC 342. Because it is one of the few galaxies bright in molecular line emission, it has extensively been used as the basis for abundance determinations of a relatively great variety of molecular species.

4.4. The center of Maffei 2

In a similar vein, rough estimates of conditions to be found in the center of Maffei 2 follow from observations of HCN, CS and other molecules: H_2 densities in the range 10^4–10^5 cm^{-3} and probably closer to the former than to the latter, as well as kinetic temperatures of about 100 K (Mauersberger et al. 1989; Hüttemeister et al. 1997; Paglione et al. 1997). The relative intensities of CO, CI, CII and the far-infrared continuum

Table 6. Beam-averaged results.

Model	Beam-averaged column densities			Total central mass		Face-on mass density		Relative mass components 1:2
	N(CO)	N(C)	$N(H_2)$	$M(H_2)$	M_{gas}	$\sigma(H_2)$	σ_{gas}	
	(10^{18} cm^{-2})		(10^{21} cm^{-2})	(10^7 $M_\odot$)		($M_\odot$/pc^{-2})		
IC 342; $N_H/N_C = 2200$; N(HI)[a] $= 1.5 \times 10^{20}$ cm^{-2}								
1	0.8	2.3	3.3	0.5	0.6	49	67	0.7 : 0.3
2	0.7	3.8	4.8	0.7	0.9	70	96	0.4 : 0.6
3	0.7	1.0	4.9	0.7	1.0	72	99	0.3 : 0.7
Maffei 2; $N_H/N_C = 2500$; N(HI)[b] $= 1.1 \times 10^{21}$ cm^{-2}								
4	1.7	1.6	3.5	0.6	0.9	28	43	0.55 : 0.45
5	3.6	1.3	5.5	0.9	1.4	43	64	0.8 : 0.2
6	2.6	1.1	4.1	0.7	1.1	32	49	0.7 : 0.3
7	2.0	1.9	4.4	0.7	1.1	32	53	0.55 : 0.45

[a] Newton (1980); [b] Hurt et al. (1996).

imply, within the context of the PDR model by Kaufman et al. (1999), somewhat higher densities close to 10^5 cm^{-3}, temperatures of about 150 K and a radiation field log $G_o = 2.3$. These temperatures and densities suggest that models 5 and 6 are more appropriate than models 4 and 7 which lack the high densities that appear to be required. Models 5 and 6 are not fundamentally different. They consist of a rather low density ($n(H_2) = 100$ cm^{-3}), hot ($T_{kin} = 100$–150 K) and very optically thick ($\tau = 15$–20 for $J = 1$–0) component and a more dense, cooler component of relatively low optical thickness. The actual temperature and density of the latter component is not firmly established. As can be seen in Table 5, temperatures between 20 and 60 K and densities between 10^4 and 10^5 cm^{-3} can be obtained by varying the relative contributions of the two gas components, requiring only that the ratio $T_{kin}^2/n(H_2)$ is kept constant. The ionized carbon intensities can only be explained by postulating the presence of a hot and dense gas phase not sampled by the CO observations but rather resulting from extensively photodissociated and ionized gas (interface with HII regions and supernova remnants?). A similar situation was found to apply in M 83 (Israel & Baas 2001).

In any case, the molecular medium in the center of Maffei 2 appears to be significantly different from that in the center of IC 342. In Maffei 2, the dense phase is warmer and probably denser, and its hot phase is much less dense. Maffei 2 is experiencing a strong central starburst comparable to the one in IC 342. A difference between the two, at least at radio wavelengths, is that Maffei 2 and M 83 have much larger amounts of nonthermal emission than IC 342 (Turner & Ho 1983, 1994). This suggests that the starbursts in Maffei 2 and M 83 are more evolved than the one in IC 342, perhaps explaining the molecular gas differences as well.

As the distance and metallicity of Maffei 2 have not been measured, we have had to assume plausible values. This is an additional source of uncertainty in the H_2 column densities, the masses and the mass densities derived for Maffei 2 in Table 6. As the observed HI column densities are much less than the model-inferred total H column densities, H_2 *column densities, masses and mass densities* scale linearly with the actual carbon abundance, whereas the H_2 and gas *masses* scale with the actual distance squared. Because it is unlikely that the distance of Maffei 2 differs much from the adopted value of 2.7 Mpc, the error in the derived mass due to this uncertainty is not more than about a factor of two. The derived X value is subject to uncertainties in the carbon abundance but not to those in the distance. The $N(H_2)$ values listed in Table 6 imply for Maffei 2 an H_2/CO conversion ratio $X = 2 - 3 \times 10^{19}$ H_2 mol cm^{-2}/K kms^{-1}, so that the same comment made for IC 342 also applies to Maffei 2.

5. Conclusions

1. Maps of the central arcminute of the nearby starburst galaxies IC 342 and Maffei 2 in various transitions of ^{12}CO and ^{13}CO, and in [CI] confirm the compact nature of the central molecular gas emission in both galaxies. Most of this gas is within a 200 parsec from the nucleus. In both galaxies, the molecular gas seems to reside in bright inner spiral arms, rather than a disk or torus.
2. Relative ^{12}CO line intensities observed in matched beams are virtually identical in IC 342 and Maffei 2. However, relative ^{13}CO intensities, as well as the intensities of the [CI] and [CII] lines differ significantly, indicating different physical conditions for the molecular gas in the two galaxies. The observed line ratios require modelling with a multi-component molecular medium in both galaxies.
3. In IC 342, a dense component with $n(H_2) \approx 10^4$ cm^{-3} and $T_{kin} \approx 10$ K is present together with a less dense $n(H_2) \approx 3 \times 10^3$ cm^{-3} and hotter $T_{kin} \approx 100$ K component. Total carbon column densities are about 1.5 times the CO column density. The modelling solution for IC 342 is reasonably well-defined.
4. In Maffei 2, the parameters of the two components minimally required are less clearly defined. The more tenuous component has $n(H_2) \approx 10^2$ cm^{-3} and $T_{kin} \approx 100$–150 K, whereas the denser component has $n(H_2) \approx 10^4$–10^5 cm^{-3} and $T_{kin} = 20$–60 K. Maffei 2 seems to be more affected by CO dissociation as it has a C/CO ratio of two to three.
5. In both starburst centers a significant fraction of the molecular mass (about half to two thirds) is associated with the hot PDR phase.

6. With an estimated gas-phase [C]/[H] abundance of order 4×10^{-4}, the centers of NGC 6946 and M 83 contain within $R = 0.25$ kpc similar (atomic and molecular) gas masses of about 10^7 $M_\odot$. Peak face-on gas mass densities are typically 70 $M_\odot\,\mathrm{pc}^{-2}$ for IC 342 and 35 $M_\odot\,\mathrm{pc}^{-2}$ for Maffei 2, but the results for the latter are subject to relatively large errors caused by uncertainties in its distance and its carbon abundance.

Acknowledgements. We are indebted to E. van Dishoeck and D. Jansen for providing us with their detailed radiative transfer models. We thank the JCMT personnel for their support and help in obtaining the observations discussed in this paper.

References

Buta, R. J., & McCall, M. L. 1999, ApJS, 124, 33
Crawford, M. K., Genzel, R., Townes, C. H., & Watson, D. M. 1985, A&A, 291, 755
Dahmen, G., Hüttemeister, S., Wilson, T. L., & Mauersberger, R. 1998, A&A, 331, 959
Downes, D., Radford, S. J., Guilloteau, S., et al. 1992, A&A, 262, 424
Dressel, L. L., & Condon, J. J. 1976, ApJS, 31, 187
Eckart, A., Downes, D., Genzel, R., et al. 1990, ApJ, 348, 434
Garnett, D. R., Shields, G. A., Skillman, E. D., Sagan, S. P., & Dufour, R. J., 1997, ApJ, 489, 63
Garnett, D. R., Shields, G. A., Peimbert, M., et al. 1999, ApJ, 513, 168
Güsten, R., Serabyn, E., Kasemann, C., et al., 1993, ApJ, 402, 537
Harris, A. I., Hills, R. E., Stutzki, J., et al. 1991, ApJ, 382, L75
Henkel, C., Mauersberger, R., & Schilke, P. 1988, A&A, 201, L23
Henkel, C., Chin, Y.-N, Mauersberger, R., & Whiteoak, J. B. 1998, A&A, 329, 443
Henkel, C., Mauersberger, R., Peck, A. B., Falcke, H., & Hagiwara, Y. 2000, A&A, 361, L45
Ho, P. T. P., Turner, J. L., & Martin, R. N. 1987, ApJ, 322, L67
Ho, P. T. P., Martin, R. N., Turner, J. L., & Jackson, J. M. 1990, ApJ, 355, L19
Huchtmeier, W. K., Karachentsev, I. D., & Karachentseva, V. E. 2000, in Small Galaxy Groups, IAU Symp. 174, ed. M.J. Valtonen & C. Flynn, ASP Conf. Ser., 209, 158
Hummel, E., & Gräve, R. 1990, A&A, 228, 315
Hurt, R. L., & Turner, J. L. 1991, ApJ, 377, 434
Hurt, R. L., Turner, J. L., Ho, P. T. P., & Martin, R. N. 1993, ApJ, 404, 602
Hurt, R. L., Turner, J. L., & Ho, P. T. P 1996, ApJ, 466, 135
Hüttemeister, S., Henkel, C., Mauersberger, R., et al. 1995, A&A, 295, 571
Hüttemeister, S., Mauersberger, R., & Henkel, C. 1997, A&A, 326, 59
Irwin, J. A., & Avery, L. W. 1992, ApJ, 388, 328
Ishiguro, M., Kawabe, R., Morita, K.-I., et al. 1989, ApJ, 344, 763
Ishizuki, S., Kawabe, R., Ishiguro, M., et al. 1990, Nature, 344, 224
Israel, F. P., White, G. J., & Baas, F. 1995, A&A, 302, 343
Israel, F. P., & Baas, F., 1999, A&A, 351, 10
Israel, F. P., & Baas, F., 2001, A&A, 371, 433
Jackson, J. M., Paglione, T. A. D., Carlstrom, J. E., & Rieu, N.-Q. 1995, ApJ, 438, 695
Jansen, D. J. 1995, Ph.D. Thesis, University of Leiden (NL)
Jansen, D. J., van Dishoeck, E. F., & Black, J. H. 1994, A&A, 282, 605
Kaufman, M. J., Wolfire, M. G., Hollenbach, D. J., & Luhman, M. L. 1999, ApJ, 527, 795
Madore, B. F., & Freedman, W. L. 1992, PASP, 104, 362
Martin, R. N., Ho, P. T. P., & Ruf, K. 1982, Nature, 296, 632
Martin, R. N., & Ho, P. T. P. 1985, ApJ, 308, L7
Mauersberger, R., & Henkel, C. 1989, A&A, 223, 79
Mauersberger, R., & Henkel, C. 1991, A&A, 245, 457
Mauersberger, R., & Henkel, C. 1993, Rev. Mod. Astron., 6, 69
Mauersberger, R., Henkel, C., & Chin, Y. N. 1995, 294, 23
Mauersberger, R., Henkel, C., Wilson, T. L., & Harju, J. 1989, A&A, 226, L5
Mauersberger, R., Henkel, C., Walsh, W., & Schulz, A. 1999, A&A, 341, 256
McCall, M. L. 1989, AJ, 97, 1341
Meier, D. S., Turner, J. L., & Hurt, R. L. 2000, ApJ, 531, 200
Meier, D. S., & Turner, J. L. 2001, ApJ, 551, 687
Morris, M., & Lo, K. Y. 1978, ApJ, 223, 803
Newton, K. 1980, MNRAS, 191, 169
Oka, T., Hasegawa, T., Hayashi, M., Handa, T., & Sakamoto, S. 1998, ApJ, 493, 370
Paglione, T. A. D., Jackson, J. M., Ishizuki, S., & Rieu, N.-Q. 1995, AJ, 109, 1716
Paglione, T. A. D., Jackson, J. M., & Ishizuki, S. 1997, ApJ, 484, 656
Petit-Pas, G. R., & Wilson, C. D. 1998, ApJ, 503, 219
Rickard, L. J., Palmer, P., Morris, M., Turner, B. E., & Zuckerman, B. 1977, ApJ, 213, 673
Rickard, L. J, & Blitz, L. 1985, ApJ, 292, L57
Rickard, L. J, & Palmer, P. M. 1981, A&A, 102, L13
Rieu, N.-Q., Henkel, C., Jackson, J. M., & Mauersberger, R. 1991, A&A, 241, L33
Rieu, N.-Q., Jackson, J. M., Henkel, C., Bach, T., & Mauersberger, R. 1992, ApJ, 399, 521
Rots, A. H. 1979, A&A, 80, 255
Sage, L. J., Shore, S. N., & Solomon, P. M. 1990, ApJ, 351, 422
Sage, L. J., & Isbell, D. W. 1991, A&A, 247, 320
Sakamoto, K., Okumura, S. K., Ishizuki, S., & Scoville, N. Z. 1999, ApJS, 124, 403
Sandage, A., & Tammann, G. A. 1987, A Revised Shapley-Ames Catalog of Bright Galaxies, second edition, Carnegie Institution of Washington Publication, 635 (Washington, D.C.: Carnegie Institution of Washington)
Sargent, A. I., Sutton, E. C., Masson, C. R., Lo, K. Y., & Phillips, T. G. 1985, ApJ, 289, 150
Sodroski, T. J., Odegard, N., Dwek, E., et al. 1995, ApJ, 452, 262
Stacey, G. J., Geis, N., Genzel, R., et al. 1985, A&A, 373, 423
Steppe, H., Mauersberger, R., Schulz, A., & Baars, J. W. M. 1990, A&A, 233, 410
Stutzki, J., Graf, U. U., Honingh, C. E., et al. 1997, ApJ, 477, L33
Takano, S., Nakai, N., Kawaguchi, K., & Takano, T. 2000, PASJ, 52, L67
Turner, J. L., & Ho, P. T. P. 1983, ApJ, 268, L79
Turner, J. L., & Ho, P. T. P. 1994, ApJ, 421, 122
Turner, J. L., & Hurt, R. L. 1992, ApJ, 384, 72
Turner, J. L., Hurt, R. L., & Hudson, D. Y. 1993, ApJ, 413, L19
van Dishoeck, E. F., & Black, J. H. 1988, ApJ, 334, 771
Vila-Costas, M. B., & Edmunds, M. G. 1992, MNRAS, 259, 121
Wall, W. F., & Jaffe, D. T. 1990, ApJ, 361, L45
Wall, W. F., Jaffe, D. T., Israel, F. P., et al. 1993, ApJ, 414, 98
Weliachew, L., Casoli, F., &, Combes, F. 1988, A&A, 199, 29
White, G. J., Ellison, B., Claude, S., Dent, W. R. F., & Matheson, D. N. 1994, A&A, 284, L23
Wright, M. C. H., Ishizuki, S., Turner, J. L., Ho, P. T. P., & Lo, K. Y. 1993, ApJ, 406, 470
Xie, S., Young, J. S., & Schloerb, F. P. 1994, ApJ, 421, 434
Young, J. S., & Sanders, D. B., ApJ, 302, 680
Young, J. S., & Scoville, N. Z. 1982, ApJ, 258, 467
Zaritsky, D., Kennicutt, R. C., & Huchra, J. P. 1994, ApJ, 420, 87